

DTIC FILE COPY

2



Naval Research Laboratory

Washington, DC 20375-5000

NRL Report 9249

AD-A219 652

Development of a Hybrid Adaptive Beamformer

F. W. LEE

*Airborne Radar Branch  
Radar Division*

February 28, 1990

DTIC  
ELECTE  
MAR 23 1990  
S E D

Approved for public release; distribution unlimited.

90 03 22 040

REPORT DOCUMENTATION PAGE			Form Approved OMB No. 0704-0188	
<small>Public reporting burden for this collection of information is estimated to average 1 hour per response, including the time for reviewing instructions, searching existing data sources, gathering and maintaining the data needed, and completing and reviewing the collection of information. Send comments regarding this burden estimate or any other aspect of this collection of information, including suggestions for reducing this burden, to Washington Headquarters Services, Directorate for Information Operations and Reports, 1215 Jefferson Davis Highway, Suite 1204, Arlington, VA 22202-4302, and to the Office of Management and Budget, Paperwork Reduction Project (0704-0188), Washington, DC 20503.</small>				
1. AGENCY USE ONLY (Leave blank)	2. REPORT DATE February 28, 1990	3. REPORT TYPE AND DATES COVERED Formal Jun 86 - May 88		
4. TITLE AND SUBTITLE Development of a Hybrid Adaptive Beamformer			5. FUNDING NUMBERS PE-62111N PR-RA11A10 DN-	
6. AUTHOR(S) F. W. Lee				
7. PERFORMING ORGANIZATION NAME(S) AND ADDRESS(ES) Naval Research Laboratory 4555 Overlook Ave., S.W. Washington, DC 20375-5000			8. PERFORMING ORGANIZATION REPORT NUMBER NRL Report 9249	
9. SPONSORING/MONITORING AGENCY NAME(S) AND ADDRESS(ES) Naval Air Development Center Warminster, PA 18974-5000			10. SPONSORING/MONITORING AGENCY REPORT NUMBER	
11. SUPPLEMENTARY NOTES				
12a. DISTRIBUTION/AVAILABILITY STATEMENT Approved for public release; distribution unlimited.			12b. DISTRIBUTION CODE	
13. ABSTRACT (Maximum 200 words) <p>Elements of adaptive array systems are reviewed and compared with the Adaptive Processing Laboratory equipment. Candidate locations for the beamforming network are investigated and development of an Intermediate Frequency Adaptive Beamformer is presented. Due to the hybrid analog/digital nature of the IF Beamformer, numerical techniques are developed for both characterization and control of the device. Performance data for the beamformer are presented.</p> <p style="text-align: right;">→ P-1</p>				
14. SUBJECT TERMS Adaptive Processing, IF Beamformer			15. NUMBER OF PAGES 25	
			16. PRICE CODE	
17. SECURITY CLASSIFICATION OF REPORT UNCLASSIFIED	18. SECURITY CLASSIFICATION OF THIS PAGE UNCLASSIFIED	19. SECURITY CLASSIFICATION OF ABSTRACT UNCLASSIFIED	20. LIMITATION OF ABSTRACT UL	

NSN 7540-01-280-5500

Standard Form 298 (Rev 2-89)  
Prescribed by ANSI Std Z39-18  
298-102

## CONTENTS

1. INTRODUCTION .....	1
2. ADAPTIVE PROCESSING LABORATORY EQUIPMENT .....	2
3. BEAMFORMING NETWORK .....	8
4. SUBSYSTEM INTEGRATION .....	11
5. SUMMARY .....	18
6. RECOMMENDATION .....	18
7. REFERF' .....	18
APPENDIX A      ation Using Linear Least Squares Fit Algorithm .....	19
APPENDIX B - Seant .....	21

Accession For	
NTIS GRA&I	<input checked="" type="checkbox"/>
DTIC TAB	<input type="checkbox"/>
Unannounced	<input type="checkbox"/>
Justification	
By _____	
Distribution/ _____	
Availability Codes <del>3</del>	
Dist	Avail and/or Special
<b>A-1</b>	



# DEVELOPMENT OF A HYBRID ADAPTIVE BEAMFORMER

fr. Form 9-88

## 1. INTRODUCTION

→ The purpose of this investigation was to develop and demonstrate the capabilities of a fully adaptive linear array beamformer. Radar systems routinely use sensor arrays for signal detection and estimation. The use of sensor arrays, instead of single sensor systems, provides radar systems the advantages of improved antenna directive gain and the ability to exploit the geometrical properties of their spatial beam patterns. One such sensor array system is an adaptive array.

→ Adaptive array systems sense the signal environment and then automatically adjust their spatial beam patterns to improve a specified performance index, usually the signal-to-interference noise ratio (SINR). These systems, therefore, perform optimally in adverse signal environments without prior knowledge of that environment. Adaptive arrays also overcome sensor failure more gracefully than conventional arrays. (See)

An adaptive array system includes three principal subsystems [1]. As illustrated in Fig. 1, these are:

- the sensor array
- the adaptive processor
- the beamforming network.

The sensor array subsystem includes the antenna elements and their receivers. The adaptive processor subsystem components are the signal processor and the weight control processor. Finally, the beamforming, or pattern-forming, network includes the element weighting and the summing network.

Section 2 describes the sensor array and the adaptive processor used for this investigation of an adaptive beamforming network. This section also describes the signal injection system used to emulate multiple mainlobe and sidelobe interference in a laboratory environment.

Section 3 examines the key component of the intermediate frequency (IF) beamforming network developed in the Adaptive Processing Laboratory.

Section 4 describes the integration of the IF beamformer to the laboratory equipment (including a discussion of the software written to control both the signal injection system and the adaptive beamformer). Performance results of the adaptive beamformer also appear in this section.

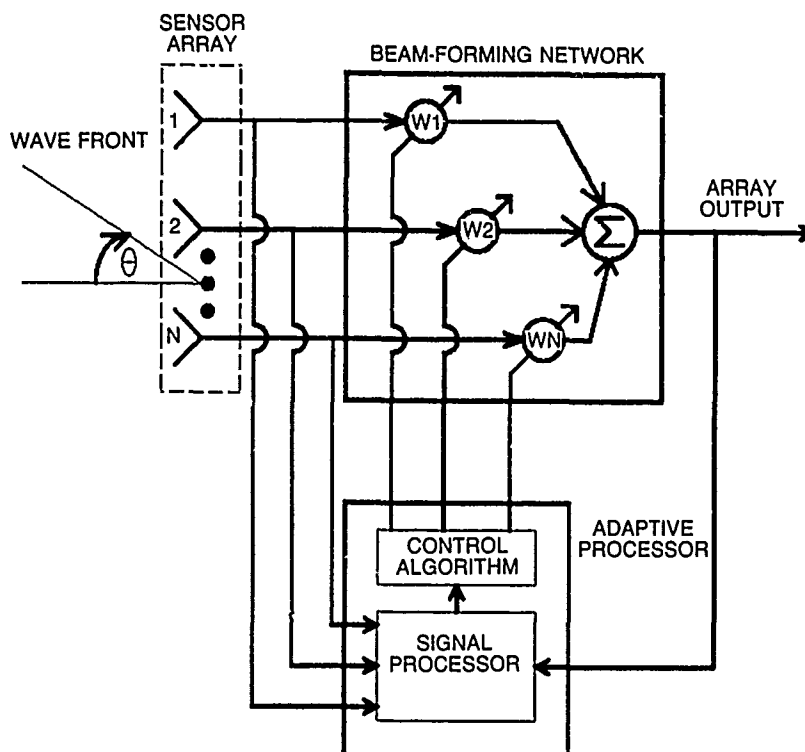


Fig. 1 - N-element adaptive array

## 2. ADAPTIVE PROCESSING LABORATORY EQUIPMENT

The laboratory equipment that comprises the sensor array and adaptive processor for this adaptive array system was part of a flight test system jointly developed by NRL and General Electric under contract number N00173-77-C-0283. In general, this system was an eight-element ultrahigh frequency (UHF) linear-array radar. The primary purpose of the flight test system was to gather clutter and electronic countermeasures (ECM) data in an airborne environment aboard an NRL P-3A aircraft. The new system uses the following flight test system components:

- the receiver group
- portions of the modified flight test radar
- the NRL recording and control group.

The receiver group (Fig. 2) consists of eight identical channels, each channel having its own receiver, IF amplifier, and synchronous demodulator. The receiver units amplify and convert the frequency of the received UHF signals to 75 MHz IF. The IF amplifiers use a surface acoustic wave (SAW) device to provide pulse compression and bandpass filtering. This unit also provides digital gain control of the amplification. Finally, the synchronous demodulator uses the 75 MHz coherent oscillator (COHO) to convert the compressed IF output to baseband inphase (I) and quadraturephase (Q) video.

The portion of the modified radar required for this experiment was the WRA 9 pulse and signal generator. This unit provides timing signals and oscillators for the entire adaptive system. It also generates the test targets and channel balance test pulse. The unit is functionally divided into eight separate elements (Fig. 3). The primary element is the timing coherent master oscillator (A2 TMG COMO). This 15 MHz crystal oscillator is the heart of all coherent operation in the system. It is multiplied in the local oscillator multiplier/select (A8

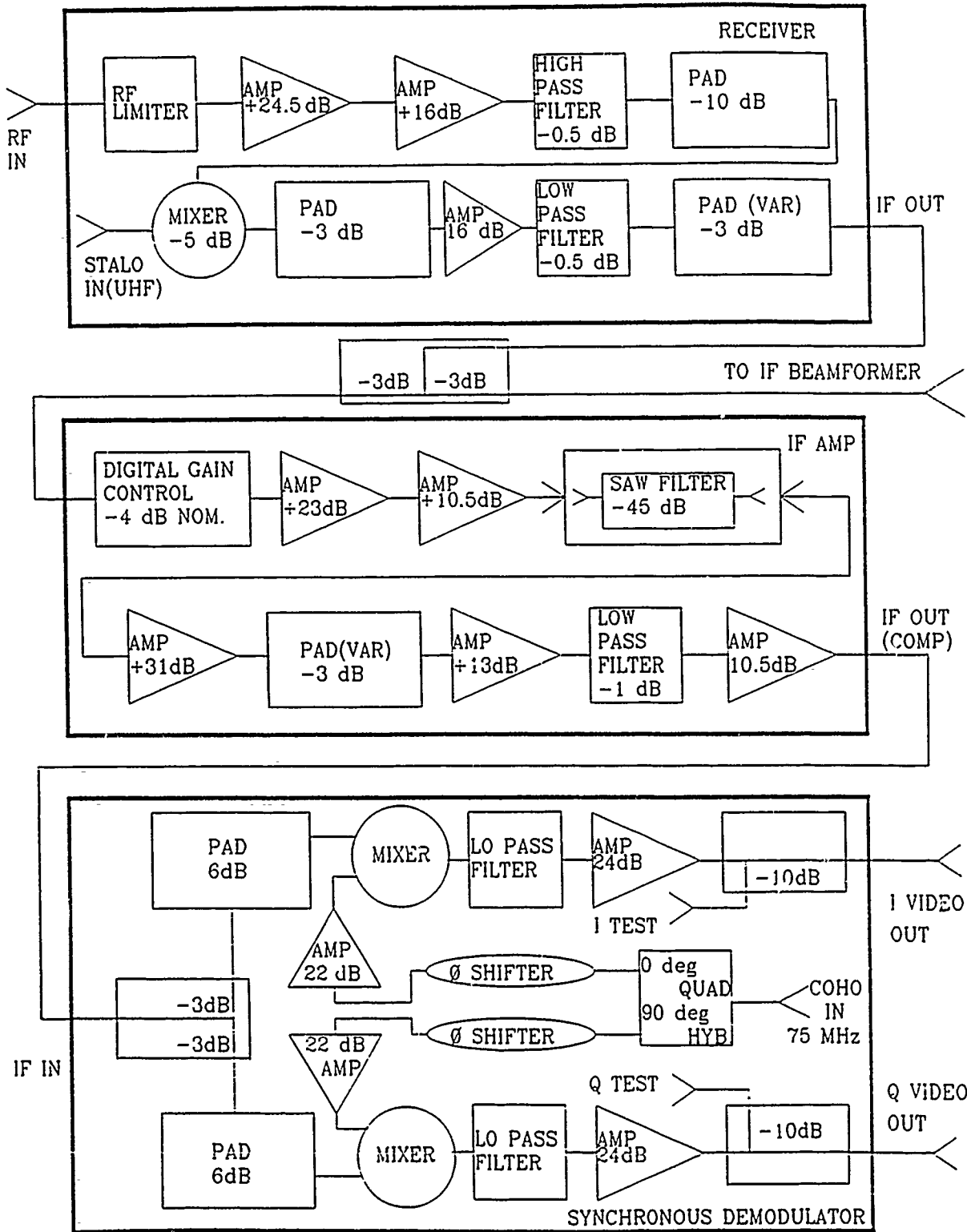


Fig. 2 - Receiver group

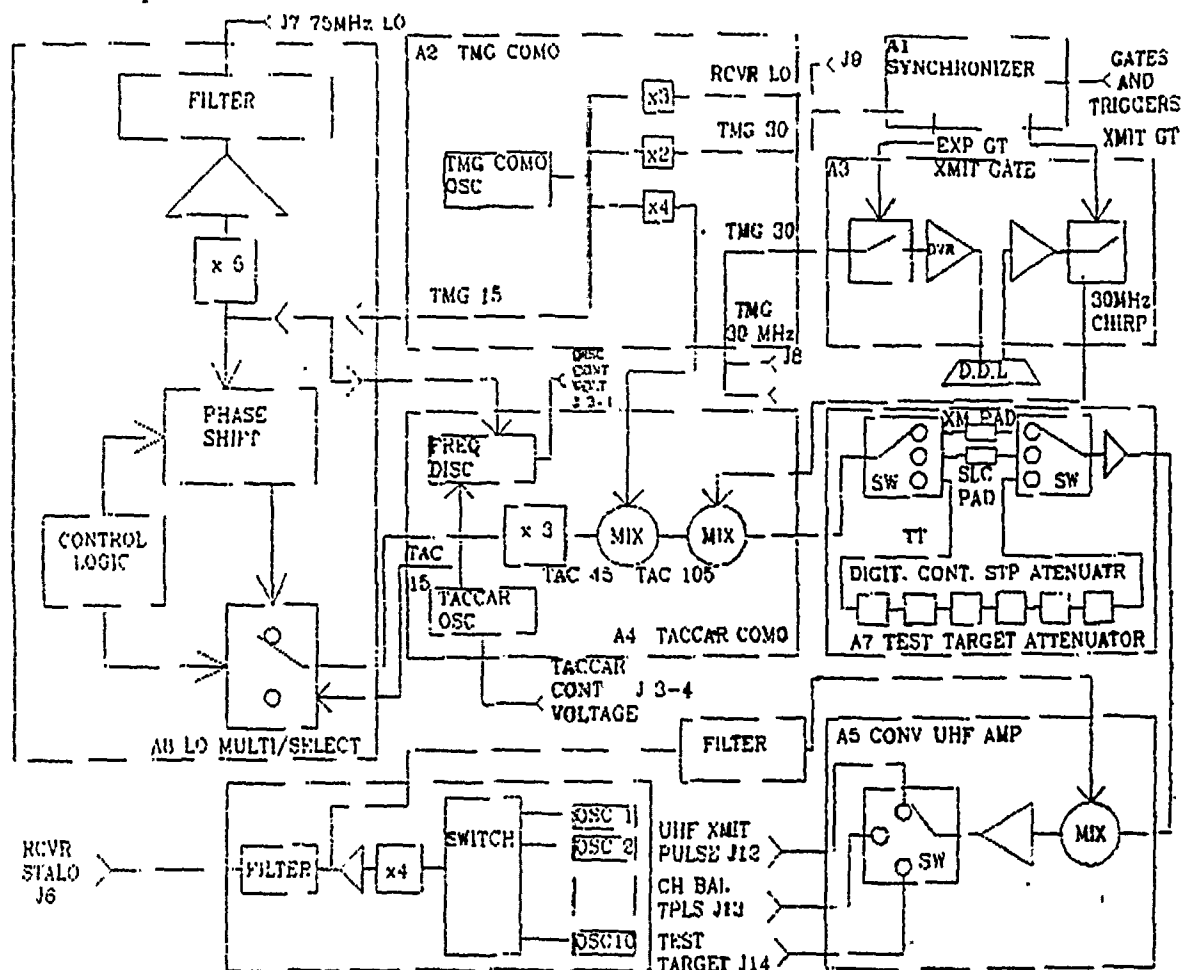


Fig. 3 - WRA 9 pulse and signal generator

LO MULTI/SELECT) to create the 75 MHz COHO. The COMO signal is also doubled to 30 MHz and sent to the transmit gate (A3 XMIT GATE), which is controlled by the synchronizer (A1), to generate the chirp waveforms used by the converter UHF amplifier (A5). The converter mixes the IF chirp waveforms with the stable local oscillator (A6 STALO) to generate the UHF transmit pulse, channel balance test pulse, and test targets. The STALO is then sent to the receivers to provide for coherent down conversion of the received signals.

The NRL recording and control group (Fig. 4) is primarily a data acquisition system optimized to acquire radar data. The basband I and Q video outputs of the synchronous demodulators in the receiver group are fed in parallel to a bank of 16 analog-to-digital (A/D) converters. The Computerlab 10 bit A/D converters are clocked by the 15 MHz COMO divided down to a 5 MHz sample rate. The digitized signals are transmitted over a 160-bit-wide data bus to a high-speed bulk memory system. The Microram 3000N memory system is used to buffer the data at the full data rate of nearly 100 megabytes per second (MB/s) and, through a custom interface, allows control over how the data are collected and sent to the Rolm 1602 computer. The data can be collected as contiguous range cells, pulses, or a combination of both. The computer can then retrieve the data for any particular radar channel or for all channels. Once in the computer, the data can either be recorded on magtape, displayed, or processed.

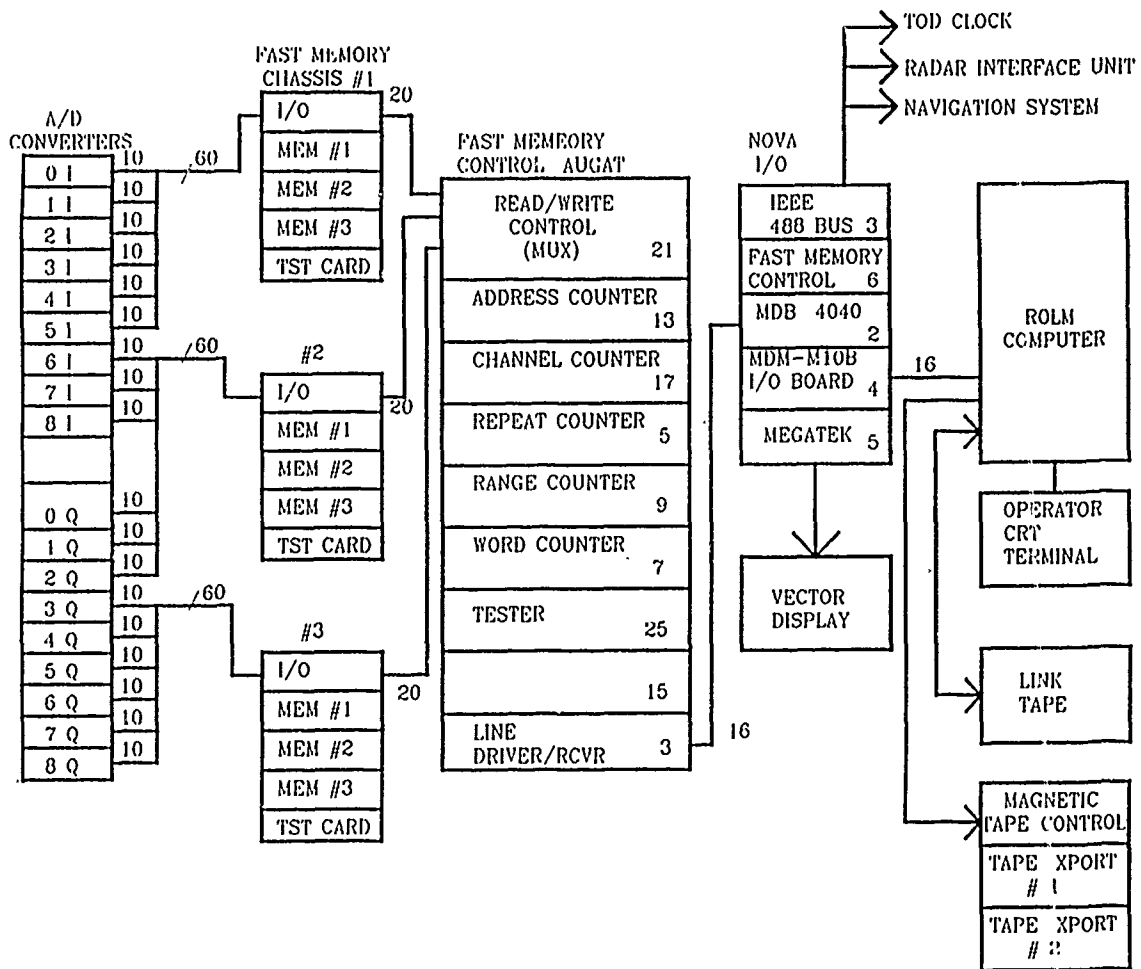


Fig. 4 - NRL recording and control group

Because of logistical problems, the transmitter and antenna used during the flight test were not incorporated into the laboratory equipment. In their place, a signal injection unit (Fig. 5) was built to emulate target returns in the presence of multiple mainlobe and sidelobe interference sources. The concept behind the signal injection unit is best illustrated by examining the geometries of a plane wave received by a linear array. A plane wave arriving from an angle  $\theta$  is received at each element of the array with an incremental phase shift caused by the individual path length difference  $d_k$  of each array element to the line of equiphase. Figure 6 expresses this phase shift in terms of the element spacing, the angle of arrival, and the wavelength of operation. The emulator mechanization (Fig. 7) of this phenomenon is accomplished by simulating the individual path length differences with coherently fed, electronically controlled phase shifters.

Merrimac PSEM-4-438B voltage-controlled phase shifters are used in the signal injection unit. They are organized in groups of eight, one for each of the eight radar channels in the system, with each group referred to as a beam. Each beam is fed by an independent source that is split by a Merrimac PDM-80-275 one-to-eight divider. Currently, the signal injection unit can control three such beams with programmable angles of arrival and a fourth beam fixed at an arrival angle of  $0^\circ$  for test signal injection. The four independent beams are then combined by channel in a Merrimac PDM-40-250 four-to-one combiner. The output is then coupled with the channel balance test pulse and test targets, which are independently controlled by manual phase shifters and attenuators for each of the eight channels. The coupled signals are injected directly into the front end of each channel's receiver. The phase shifter control voltages are supplied by digital-to-analog (D/A) converter cards in the Hewlett-Packard Multiprogrammer (which interfaces and is controlled by the Rolm 1602 computer). This

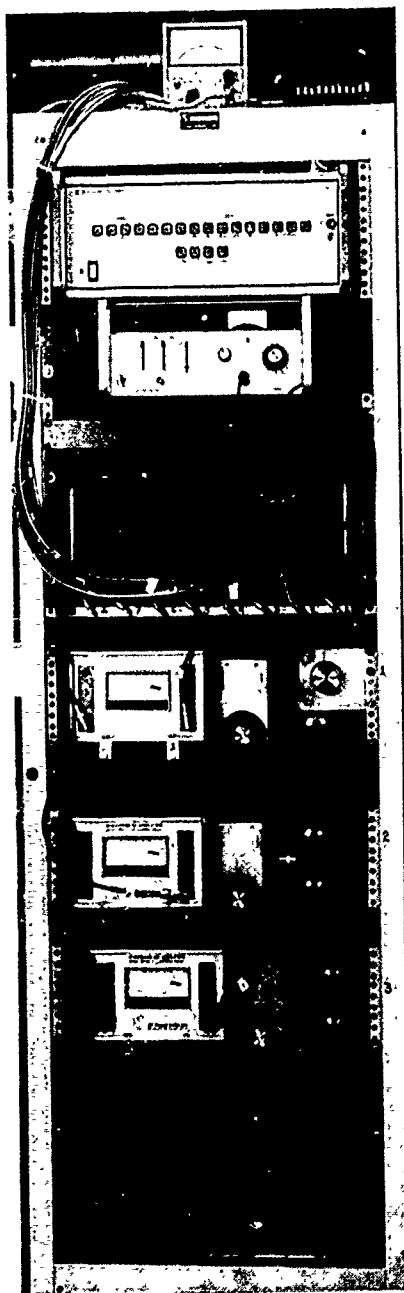


Fig. 5 - Signal Injection Unit (SIU)

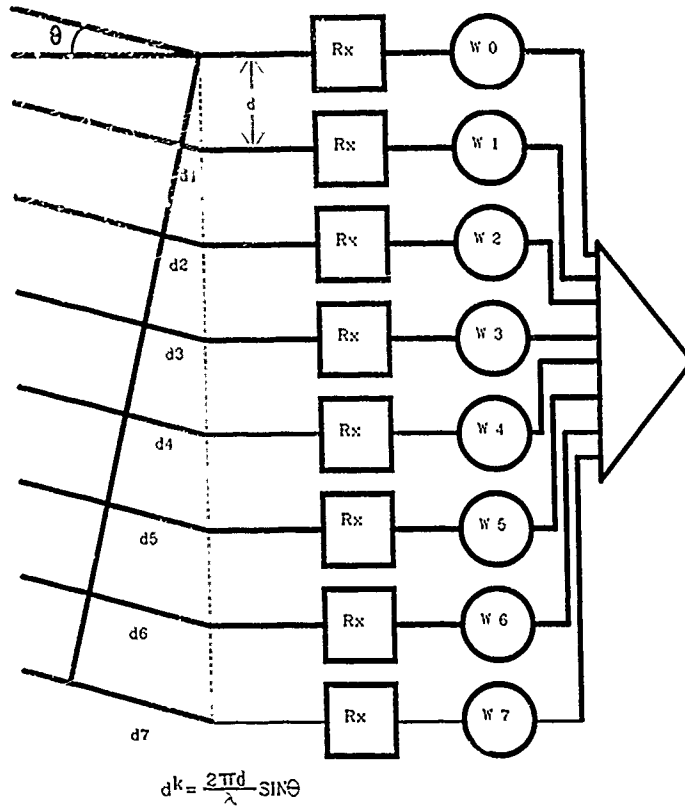


Fig. 6 - Plane wave geometry

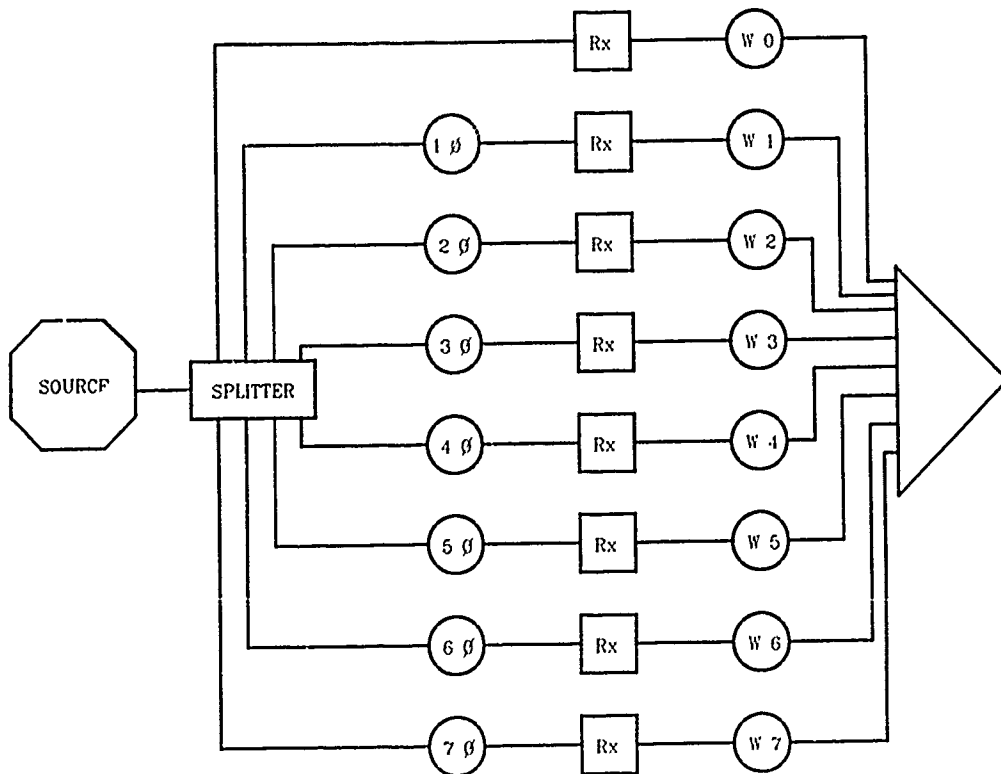


Fig. 7 - Emulator mechanization

configuration allows for closed loop operation between the sampling system and the signal injection unit. Figure 8 diagrams the signal injection unit.

Using the bisection algorithm, NRL researchers developed control software to set up the beams for a desired angle of arrival. This algorithm, sometimes referred to as the binary-search method, is based on the Intermediate Value Theorem [2] which states that for any given function  $F$ , continuous between the interval  $[a,b]$  and  $K$  is any number between  $F(a)$  and  $F(b)$ , there exists  $c$  in  $(a,b)$  for which  $f(c)=K$ . In the case of the phase shifters, the system can be thought of as the function  $F$  and the desired phase shift as  $K$ .

The algorithm attempts to find the voltage  $c$  to establish the desired phase shift. After setting the control voltages on all channels, the program checks the actual phase shifts against the calculated phase shifts to determine its phase error performance. Typical phase errors are on the order of  $\pm 3^\circ$  and can be attributed to the .06 V quantization step of the D/A converters.

### 3. BEAMFORMING NETWORK

Section 2 deals with two of the three primary subsystems of the adaptive array. In Section 3, the beamforming network is detailed. The beamforming network multiplies the output of each sensor by a complex weight, providing for both amplitude and phase control, and then adds the output to all other weighted sensor outputs of the array. Mathematically, this can be described as performing a vector dot product of the channel vector with the weighting vector. It is at this point in the system that the antennas' spatial beam pattern is determined.

There are three candidate locations for performing the pattern-forming task in this particular adaptive array system:

- prior to the receiving group
- on the digitized video signals
- on the IF section of the receiving chain.

The first possible location for the pattern-forming network is just prior to the receiver group. This point, which in an operational system would be just after the antenna elements, is the classical point at which arrays with fixed beam patterns are formed. The major asset to conventional arrays of forming the beam at this point is that only one receiving channel is required. Adaptive arrays, however, must be able to sense the signal environment of all the elements; therefore, a receiver chain for each sensor is needed regardless of whether the beam is formed at this point or at some other point further down the chain. Another drawback to locating the beamforming network prior to the receivers is the difficulty in constructing an accurate weighting network capable of wideband operation. The wideband requirement is placed on the network by the multifrequency channel capability of this system.

The second candidate beamforming location is after the A/D converters have digitized the I and Q video outputs of the synchronous demodulators (i.e., at the end of the receiver chain). The main advantages to forming the beam on the digital signals is that the weighting network is identical channel to channel and the phase and amplitude control of the now digital complex phase multipliers are independent of frequency. The major drawback to such a system is its overall complexity caused by the necessary computational throughput of the beamforming processor. This type of beamformer is currently being investigated as a possible alternative to the analog beamformer because of the recent development of digital signal processing (DSP) integrated circuits.

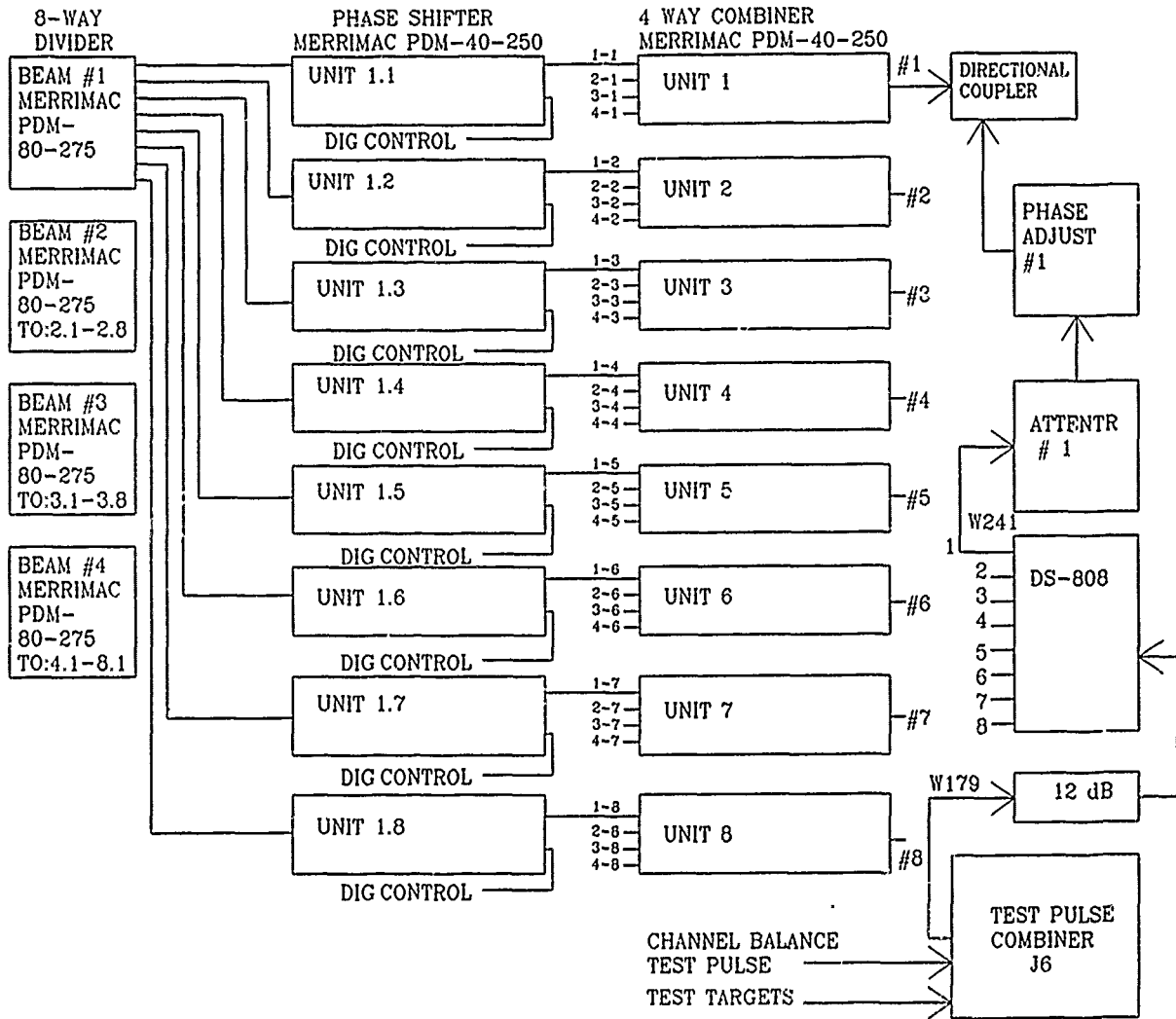


Fig. 8 - SIU block diagram

The IF section of the receiving chain is the final candidate location for the beamforming network and, as stated in the introduction, it is the type of beamformer developed for this investigation. This portion of the chain immediately follows the receivers and is accessible as either preamplified uncompressed IF directly out of the receiver or postamplified compressed IF following the dispersive filters. Of these two choices of IF signals, the preamplified uncompressed IF is the more suitable for beamforming because of its superior channel match compared to the postamplified compressed IF. The General Electric specification on the channel matching capabilities of the receivers is 40 dB minimum with 43 dB typically measured [3]. This performance exceeds by 10 dB the minimum and typical channel match of the Autonetics 75 MHz SAW dispersive delay lines used in the dispersive filters [4]. Since frequency-dependent interchannel mismatch across the cancellation bandwidth is a principal array characteristic governing the degree of interference signal cancellation that an adaptive array can achieve, the preamplified uncompressed IF section was chosen for the location of the beamforming network.

The key component chosen for the IF beamformer was the Olckron O-CPM-70 complex phasor modulator. The complex phasor modulator's circuit (Fig. 9) is similar to that of a standard single sideband modulator. The

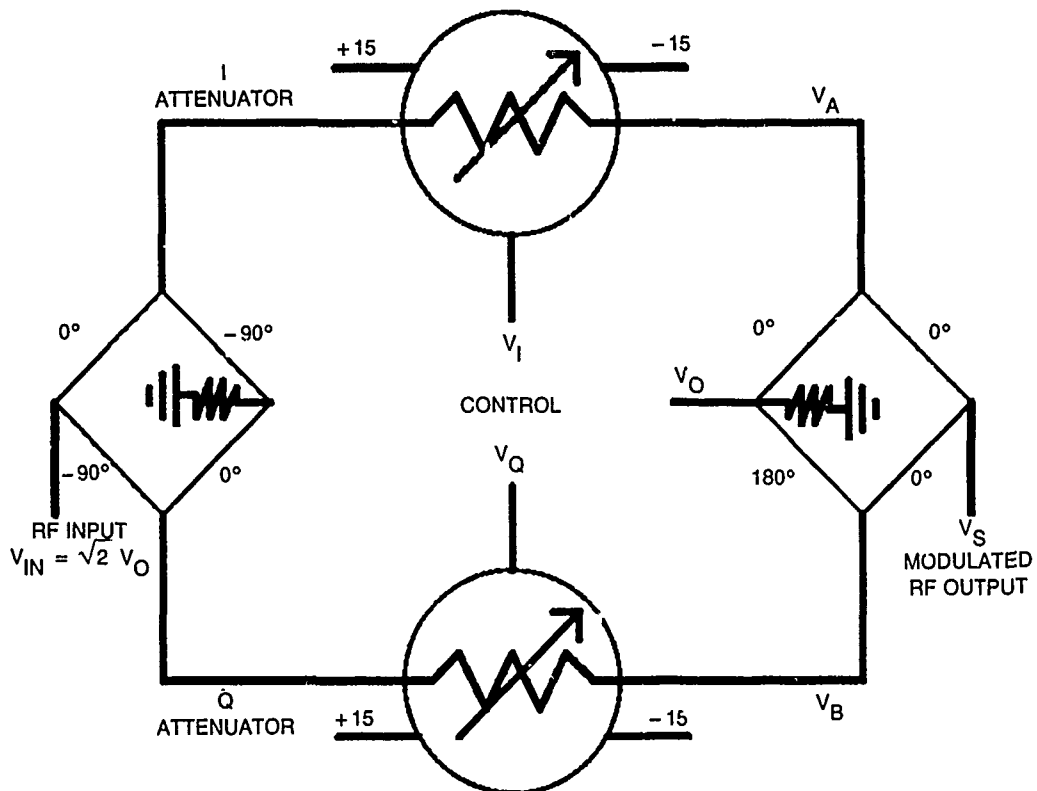


Fig. 9 - CPM circuit diagram

difference is that the single sideband modulator's double-balanced mixers are replaced by a pair of voltage-controlled attenuators [5]. The basic characteristics of the CPM as a function of the input phasor  $V_{in}$  and the control voltages  $V_I$  and  $V_Q$  are described by the following relationships:

$$V_{IN} = 2 V_O$$

$$V_I = V_c \cos \theta$$

$$V_Q = V_c \sin \theta$$

$$V_S = (KV_c / 2) * V_O e^{-j\theta} \quad K = \text{scale factor}$$

The I and Q control voltages have a linear range of  $\pm 2$  V and modulation bandwidths of approximately 50 kHz. The CPMs were tested to determine their phase and amplitude linearity with respect to a 15 x 15 square control voltage grid by using constellation analysis. Referring to Fig. 10, the control voltages  $V(I)$  and  $V(Q)$  vary uniformly from -1.4 to +1.4 V in .2 V steps. The phase and amplitude of the CPM's output is measured and plotted in polar coordinates. Ideally, the mesh connecting each of these points would be as uniform as the control voltage grid (not shown). The results of the tests were evaluated and, based on the relatively linear response to the control voltage grids, a linear least squares fit in two variables was chosen as the algorithm to characterize and control the devices. This software is discussed in more detail in Section 4.

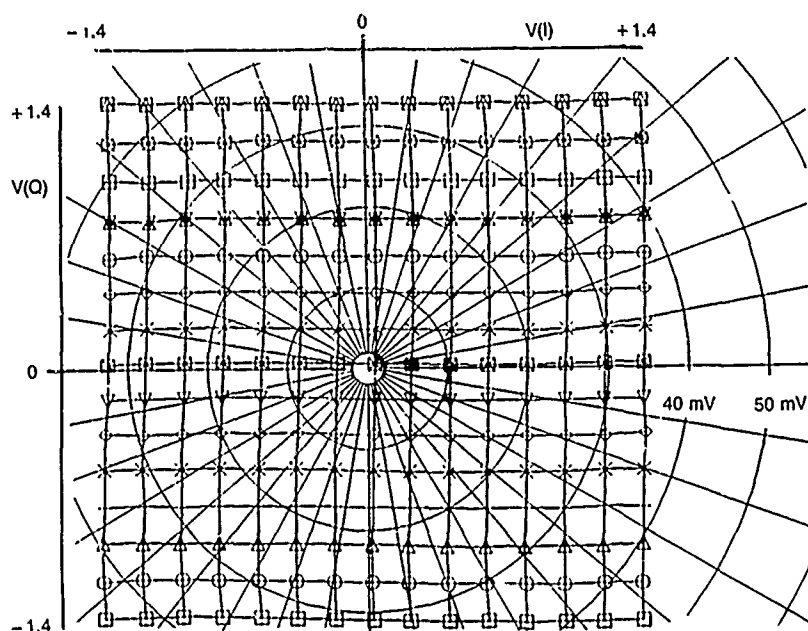


Fig. 10 - Complex Phase Modulator response as a function of control voltages

#### 4. SUBSYSTEM INTEGRATION

Interfacing the IF Beamformer (Fig. 11) into the Adaptive Array System was a relatively uncomplicated task. The original flight test system had formed a broadside beam in the IF section by splitting the inputs to the dispersive filters and installing a set of fixed attenuators with attenuation values chosen for a 25 dB Dolph-Tschebyscheff beam pattern. The outputs of the attenuators were summed in an eight-to-one combiner and then fed to a dispersive filter, synchronous detector, and a pair of A/D converters. The digital output was stored in the same high-speed bulk memory system described in Section 2. To integrate the IF beamformer into the system, all that was required was to replace the attenuators with the IF beamformer and some additional cabling. Figure 12 is the block diagram of the Adaptive Array Laboratory System. The I and Q control voltages required by the CPMs are supplied by additional D/A converters from the H-P Multiprogrammer.

The more difficult task in completing the integration was to develop the software to control the IF beamformer. Figure 1 shows that the adaptive processor is composed of a control algorithm and a signal processor. The control algorithm handles the setting of the complex weights. The signal processor samples the sensor array and the array output, and it uses an adaptive algorithm to determine the weights to send to the control algorithm.

The software developed for the IF beamformer was partitioned into two tasks. The first task was to develop the control algorithm to set the weights for the quiescent and adapted beams. As stated before, the outcome of the constellation analysis was to use a linear least squares fit in two variables to characterize the response of each CPM to the square control voltage grid. This algorithm, detailed in Appendix A, calculates for each channel a two-by-two matrix as well as I and Q dc offsets such that the following matrix relationship holds:

$$\begin{bmatrix} C_I \\ C_Q \end{bmatrix} = \begin{bmatrix} A_{11} & A_{12} \\ A_{21} & A_{22} \end{bmatrix} * \begin{bmatrix} X - I_{dc} \\ Y - Q_{dc} \end{bmatrix}$$

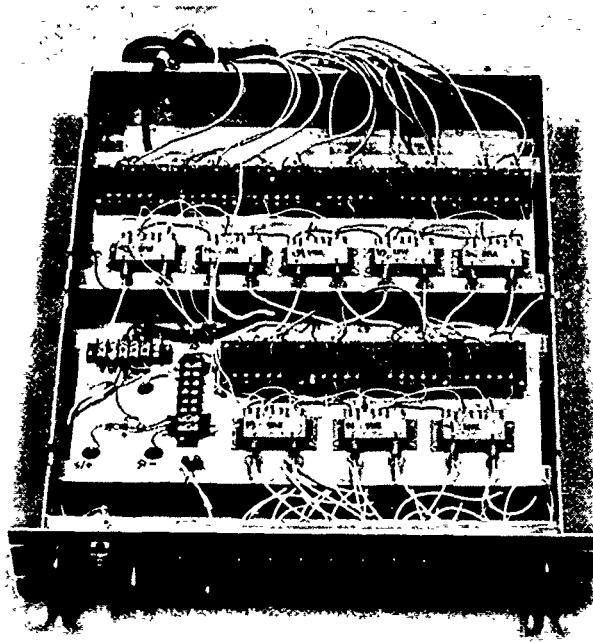


Fig. 11 - IF beamforming network

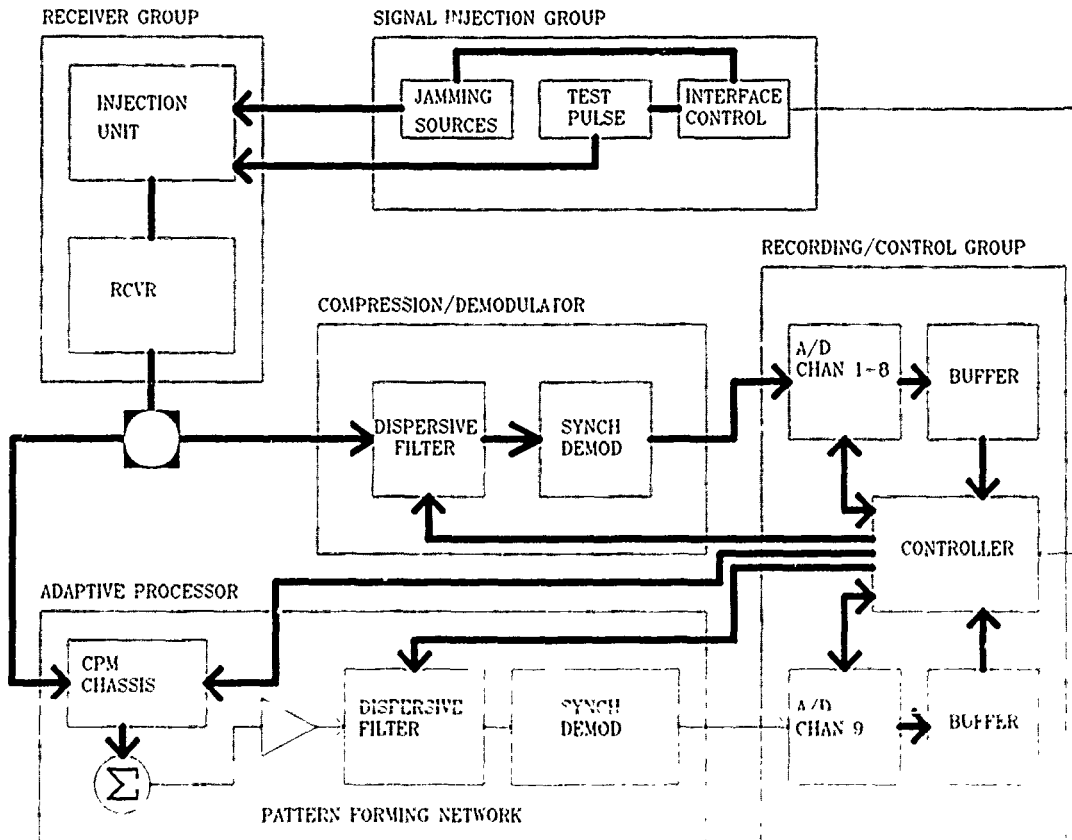


Fig. 12 - Block diagram of the adaptive array laboratory system

The X and Y in this matrix equation comprise the desired normalized complex weight for a particular channel through the beamforming path. If, for example, the values for (X,Y) were specified to be (1,0) for channel 1, this equation would yield the two voltage control words  $C_I$  and  $C_Q$  necessary to send to the Multiprogrammer such that the CPM for channel 1 would weight the signal to be equal in amplitude and phase to that of the through path. To further emphasize this point, if (X,Y) were specified to be (0,1), then the voltage control words would weight the signal to be equal in amplitude and  $90^\circ$  out of phase with that of the through path. To test this method of setting the weights, a computer program was developed to electronically scan the mainlobe of the beamformer from  $-90^\circ$  to  $+90^\circ$  with a CW signal injected at an angle of  $0^\circ$ . Null depths of 30 dB were measured with respect to the mainbeam. In Section 3, the receivers are specified to be matched to within 40 dB across the entire receiver bandwidth. Such a loss in performance was deemed unacceptable and it was reasoned that the performance of the beamformer was limited by the accuracy to which the desired weights were set.

To improve the accuracy of setting the weights, a closed loop technique, known as the Secant Method, was used. The Secant Method (Appendix B) is based on the Newton-Raphson Method for solving a root-finding problem and has the advantage over the linear least squares fit in that it is an iterative method with a feedback term. This term allows the method to compensate for errors present in the weight setting, converging the control voltages to their optimum values to establish the desired weight. The only drawback to this algorithm is that convergence is not always guaranteed unless good approximations for the control voltages are known at the start of the process [6]. Therefore, the Secant Method is used to refine the solutions for the control voltages provided by the least squares algorithm.

By use of the same mainbeam scanning computer program as mentioned before, now with the improved weight setting algorithms, new data were collected. Figure 13 shows typical measurements of the output power of the IF beamformer. The null depths have been vastly improved to greater than 50 dB, and the measured beam patterns closely resemble theoretical Tschebyscheff patterns. The perturbations visible on the sidelobes of the beam patterns can be attributed to the 4 mV step of the controlling D/A converters.

The second task, generically referred to as the signal processor, handles the data acquisition and calculation of the adaptive weights to send to the above-mentioned control algorithm. Although numerous adaptive algorithms exist for calculating these weights, all the algorithms can be classified as either closed loop, feedback algorithms or open loop, feedforward algorithms. An algorithm from each class was coded to test the beamformer's performance against simulation results. The closed loop algorithm chosen was the classic Howells-Applebaum adaptive loop and the open loop algorithm was the Direct Sampled Matrix Inverse.

The Howells-Applebaum adaptive loop was first investigated in the early 1960s and was initially applied as an analog signal processor to an IF radar sidelobe canceller [7]. The basic loop (Fig. 14) is composed of six components with each of the eight channels of the array requiring such a loop. Of these six components, the phase conjugator, correlator, integrator, and differential amplifier were all implemented in this investigation as models of their analog counterparts in the control computer. The IF beamformer with the CPM devices and an eight-to-one combiner completed the hybrid analog/digital system required to implement the Howells-Applebaum Adaptive Processor. Applebaum [8] established a rigorous mathematical analysis of the control-law governing the operation of this adaptive loop. The basic iterative mathematical expression governing this is:

$$W^k = G/\tau S^* - (G/\tau M^k - I(1-1/\tau)) W^{k-1},$$

where

$$M^k = V^{k*} V_T^k.$$

Table 1 presents typical results for this algorithm. Figure 15 shows the beam patterns measured for the corresponding quiescent and adapted weight vectors. Oscilloscope photographs of the video output of the IF

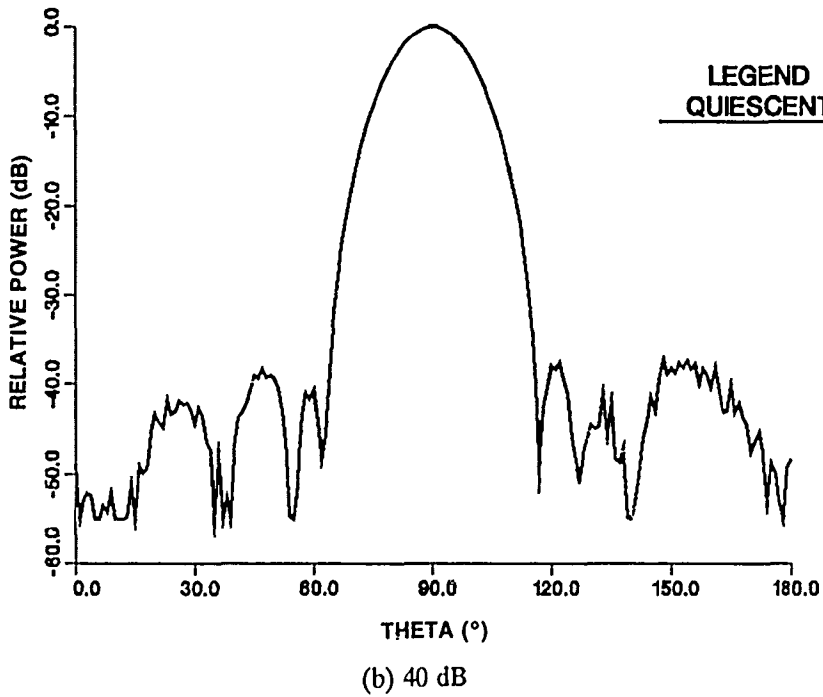
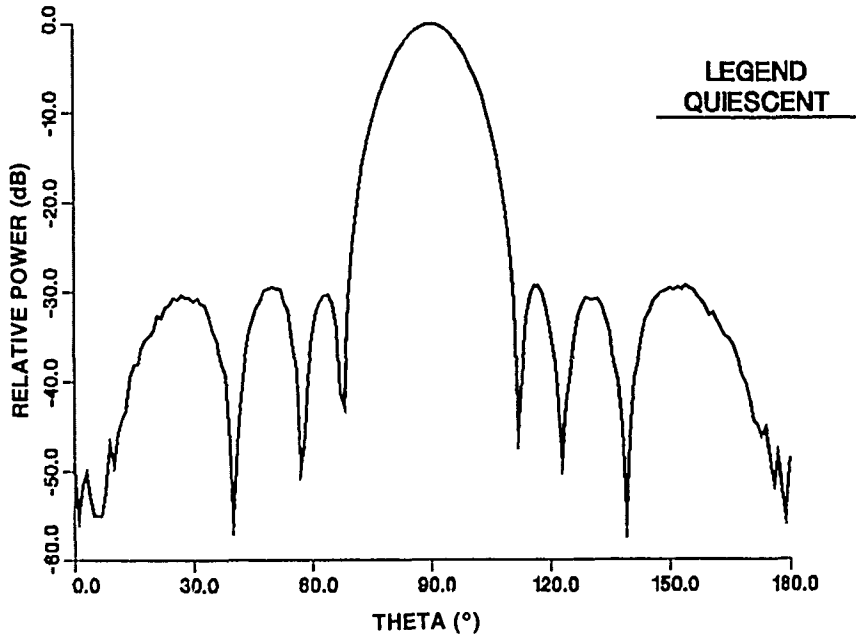


Fig. 13 - Tschebyscheff beam patterns

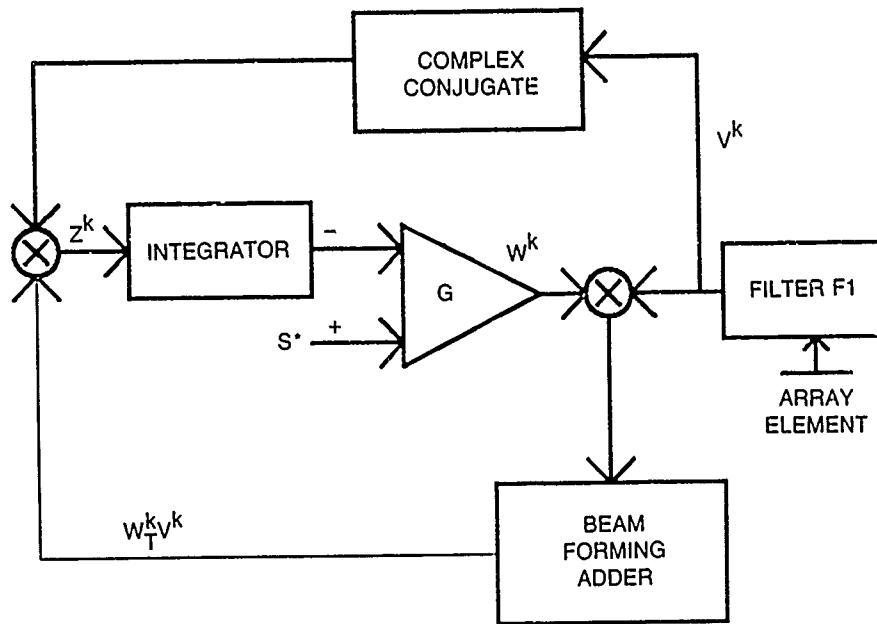


Fig. 14 - Howells-Applebaum adaptive loop

Table 1 -- Typical Performance Data

1. MEASURED QUIESCENT OUTPUT	
$P_S = -23.77$ dB	
$P_I = -20.39$ dB	
$SINR_B = P_S - P_I = -3.38$ dB	
2. MEASURED ADAPTED OUTPUT	
$P_S = -23.98$ dB	
$P_I = -39.96$ dB	
$SINR_A = P_S - P_I = 15.98$ dB	
3. IMPROVEMENT FACTOR	
$SINR_A - SINR_B = 19.36$ dB	

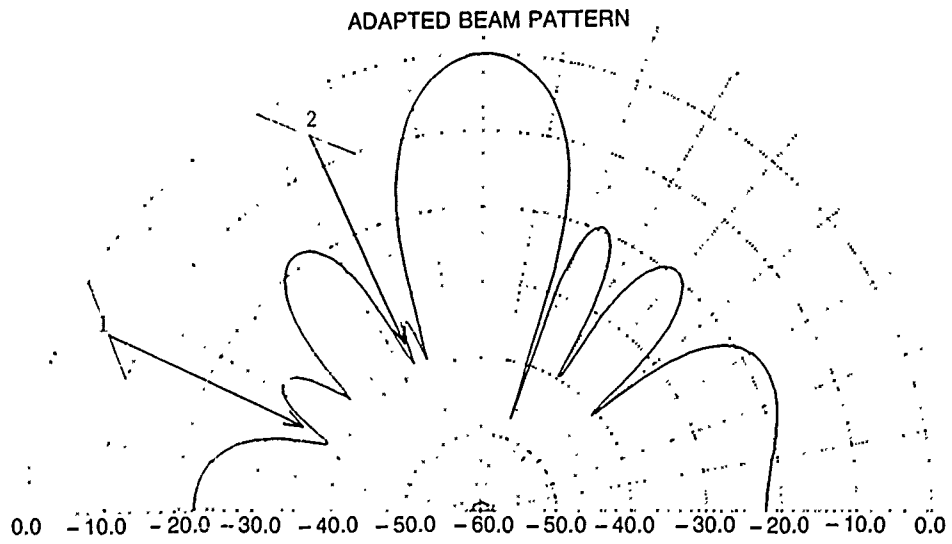
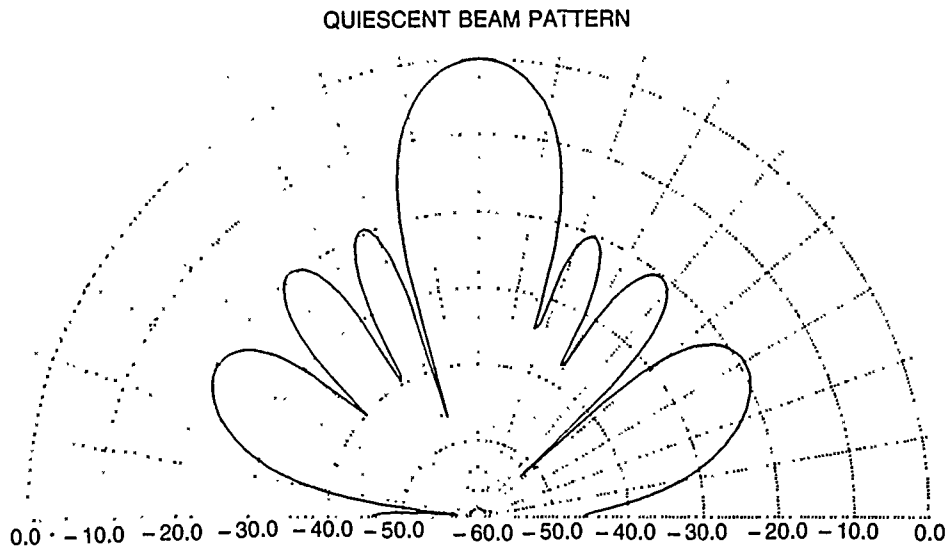


Fig. 15 - Beam patterns measured for the corresponding quiescent and adapted weight vectors

as an estimate of the actual covariance matrix, the algorithm performs a matrix inversion using Gaussian Elimination. The optimum Wiener weights that are sent to the weight control processor are derived from multiplying the inverse matrix by the steering vector. Because this algorithm was meant to test the effectiveness of the beamformer on open loop algorithms, no error feedback for weight correction was used. The major reason that this algorithm failed can be attributed to both the error in setting the calculated weights and the precision of the computer system used to calculate the inverse of the sampled covariance matrix.

## 5. SUMMARY

This report details the equipment and capabilities of the Adaptive Processing Laboratory for implementing and testing various adaptive algorithms. An Intermediate Frequency Beamformer was developed and integrated with existing laboratory equipment to complete the fully adaptive system. This system proved to be most effective for implementing and testing closed loop adaptive algorithms. However, fundamental control problems with the complex phase modulators, the primary analog signal processing components chosen for the IF beamformer, do not allow successful implementation of open loop adaptive algorithms.

## 6. RECOMMENDATION

Since the IF beamformer does not successfully lend itself to open loop algorithms, it is recommended that a completely digital beamformer be developed. With the recent advances in digital signal processing technologies, a digital beamformer capable of applying complex weights and accumulation of the digitized voltages at a sustained rate equal to the sample rate of the A/D converters is possible and would allow for more detailed investigation into the performance of open loop adaptive algorithms and superresolution techniques in a real-time system.

## 7. REFERENCES

1. R. Monzingo and T. Miller, Introduction to Adaptive Arrays (Wiley-Interscience, New York, 1980), Ch. 1.
2. R. Burden and J. D. Faires, Numerical Analysis (Prindle, Weber & Schmidt, Boston, 1985), Ch. 1.
3. J. F. Sweeney, "Adaptive Array Receiver Component Evaluation. Part I. Synchronous Demodulator and Radome Receiver Module," General Electric Company, Report NRL-TR-77, May 31, 1977.
4. I. K. McLennan, "Adaptive Array Receiver Component Evaluation. Part II. Dispersive Filter with Discrete Gain Control," General Electric Company, Report NRL-TR-78, Oct. 1978.
5. J. P. Curtis, "Complex Phasor Modulators Control Amplitude and Phase Simultaneously," Microwaves & RF, July 1983, pp. 123-124.
6. R. Burden and J. D. Faires, Numerical Analysis (Prindle, Weber & Schmidt, Boston, 1985), pp. 42-48.
7. P. W. Howells, "Intermediate Frequency Side-Lobe Canceller," U.S. Patent 3202990, Aug. 24, 1965.
8. S. P. Applebaum, "Adaptive Arrays," Syracuse University Research Corp., Report SPL TR 66-1, Aug. 1966; Reprinted in IEEE Trans. Antennas Propag. AP-24, 585-598, Sept. 1976.

## Appendix A

### CALIBRATION USING LINEAR LEAST SQUARES FIT ALGORITHM

Purpose:

This calibration method uses the Linear Least Squares Fit Algorithm to compute a 2 x 2 transform matrix to transform a desired normalized weight into the necessary control voltages to achieve the desired amplitude and phase with respect to a Reference channel.

Inputs:

- $R_{Ij}$  = Reference Channel Inphase Voltage
- $R_{Qj}$  = Reference Channel Quadrature-phase Voltage
- $T_{Ij}$  = Test Channel Inphase Voltage
- $T_{Qj}$  = Test Channel Quadrature-phase Voltage
- $N$  = Total Number of Samples

Calculate:

For  $k=1, n \times n$  and  $j=1, N$

$$N \cdot X_k := \sum_j R_{Ij} \cdot T_{Ij} + \sum_j R_{Qj} \cdot T_{Qj} \quad X_k := \frac{X_k}{R_k}$$

$$N \cdot Y_k := \sum_j R_{Qj} \cdot T_{Ij} - \sum_j R_{Ij} \cdot T_{Qj} \quad Y_k := \frac{Y_k}{R_k}$$

$$N \cdot R_k^2 := \sum_j R_{Ij}^2 + \sum_j R_{Qj}^2$$

Assume  $n \times n$  Command Matrix with Command words

$$C_I + j \cdot C_Q$$

$$\bar{x} := \frac{1}{n^2} \cdot \sum_k X_k \quad \bar{Y} := \frac{1}{n^2} \cdot \sum_k Y_k \quad \alpha := \frac{1}{n^2} \cdot \sum_k C_{Ik}$$

$$S_{II} := \sum_k X_k \cdot C_{Ik} \quad S_{IQ} := \sum_k X_k \cdot C_{Qk}$$

$$S_{QI} := \sum_k Y_k \cdot C_{Ik} \quad S_{QQ} := \sum_k Y_k \cdot C_{Qk}$$

$$SS_I := \sum_k X_k^2 \quad SS_Q := \sum_k Y_k^2$$

$$\beta := \frac{\alpha}{S_{II} \cdot S_{QQ} - S_{IQ} \cdot S_{QI}}$$

The 2 x 2 Transform matrix coefficients are:

$$A_{11} := \beta \cdot S_{QQ} \quad A_{12} := \beta \cdot S_{IQ}$$

$$A_{21} := \beta \cdot S_{QI} \quad A_{22} := \beta \cdot S_{II}$$

## Appendix B

### SECANT ALGORITHM

Purpose:

This method finds a solution to  $f(x) = 0$  given initial approximations  $P_0$  and  $P_1$  and  $x$  is a complex variable and  $f(x)$  is a complex function.

Set

$i := 2$                        $N_0$  = maximum number of iterations  
 $q_0 := f(P_0)$   
 $q_1 := f(P_1)$                  $TOL$  = tolerance

While  $i < N_0$

$$P := P_1 - q_1 \cdot \frac{P_1 - P_0}{q_1 - q_0}$$

If  $|P - P_1| < TOL$  then procedure completed successfully

$i := i + 1$

Set

$P_0 := P_1$   
 $q_0 := q_1$   
 $P_1 := P$   
 $q_1 := f(p)$

Continue until maximum number of iterations exceeded